HEP/123-qed
Fermilab FERMILAB-Pub-00/101-E CDF October 2000

Measurement of the Top Quark p_T Distribution

(May 10, 2000)

T. Affolder,[21] H. Akimoto,[43] A. Akopian,[36] M. G. Albrow,[10] P. Amaral,[7] S. R. Amendolia,[32] D. Amidei,[24] K. Anikeev,[22] J. Antos,[1] G. Apollinari,[10] T. Arisawa,[43] T. Asakawa,[41] W. Ashmanskas,[7] M. Atac,[10] F. Azfar,[29] P. Azzi-Bacchetta,[30] N. Bacchetta,[30] M. W. Bailey,[26] S. Bailey,[14] P. de Barbaro,[35] A. Barbaro-Galtieri,[21] V. E. Barnes,[34] B. A. Barnett,[17] M. Barone,[12] G. Bauer,[22] F. Bedeschi,[32] S. Belforte,[40] G. Bellettini,[32] J. Bellinger,[44] D. Benjamin,[9] J. Bensinger,[4] A. Beretvas,[10] J. P. Berge,[10] J. Berryhill,[7] B. Bevensee,[31] A. Bhatti,[36] M. Binkley,[10] D. Bisello,[30] R. E. Blair,[2] C. Blocker,[4] K. Bloom,[24] B. Blumenfeld,[17] S. R. Blusk,[35] A. Bocci,[32] A. Bodek,[35] W. Bokhari,[31] G. Bolla,[34] Y. Bonushkin,[5] D. Bortoletto,[34] J. Boudreau,[33] A. Brandl,[26] S. van den Brink,[17] C. Bromberg,[25] M. Brozovic,[9] N. Bruner,[26] E. Buckley-Geer,[10] J. Budagov,[8] H. S. Budd,[35] K. Burkett,[14] G. Busetto,[30] A. Byon-Wagner,[10] K. L. Byrum,[2] P. Calafiura,[21] M. Campbell,[24] W. Carithers,[21] J. Carlson,[24] D. Carlsmith,[44] J. Cassada,[35] A. Castro,[30] D. Cauz,[40] A. Cerri,[32] A. W. Chan,[1] P. S. Chang,[1] P. T. Chang,[1] J. Chapman,[24] C. Chen,[31] Y. C. Chen,[1] M. -T. Cheng,[1] M. Chertok,[38] G. Chiarelli,[32] I. Chirikov-Zorin,[8] G. Chlachidze,[8] F. Chlebana,[10] L. Christofek,[16] M. L. Chu,[1] C. I. Ciobanu,[27] A. G. Clark,[13] A. Connolly,[21] J. Conway,[37] J. Cooper,[10] M. Cordelli,[12] J. Cranshaw,[39] D. Cronin-Hennessy,[9] R. Cropp,[23] R. Culbertson,[7] D. Dagenhart,[42] F. DeJongh,[10] S. Dell'Agnello,[12] M. Dell'Orso,[32] R. Demina,[10] L. Demortier,[36] M. Deninno,[3] P. F. Derwent,[10] T. Devlin,[37] J. R. Dittmann,[10] S. Donati,[32] J. Done,[38] T. Dorigo,[14] N. Eddy,[16] K. Einsweiler,[21] J. E. Elias,[10] E. Engels, Jr.,[33] W. Erdmann,[10] D. Errede,[16] S. Errede,[16] Q. Fan,[35] R. G. Feild,[45] C. Ferretti,[32] R. D. Field,[11] I. Fiori,[3] B. Flaugher,[10] G. W. Foster,[10] M. Franklin,[14] J. Freeman,[10] J. Friedman,[22] Y. Fukui,[20] I. Furic,[22] S. Galeotti,[32] M. Gallinaro,[36] T. Gao,[31] M. Garcia-Sciveres,[21] A. F. Garfinkel,[34] P. Gatti,[30] C. Gay,[45] S. Geer,[10] D. W. Gerdes,[24] P. Giannetti,[32]

P. Giromini,[12] V. Glagolev,[8] M. Gold,[26] J. Goldstein,[10] A. Gordon,[14] A. T. Goshaw,[9] Y. Gotra,[33] K. Goulianos,[36] C. Green,[34] L. Groer,[37] C. Grosso-Pilcher,[7] M. Guenther,[34] G. Guillian,[24] J. Guimaraes da Costa,[14] R. S. Guo,[1] R. M. Haas,[11] C. Haber,[21] E. Hafen,[22] S. R. Hahn,[10] C. Hall,[14] T. Handa,[15] R. Handler,[44] W. Hao,[39] F. Happacher,[12] K. Hara,[41] A. D. Hardman,[34] R. M. Harris,[10] F. Hartmann,[18] K. Hatakeyama,[36] J. Hauser,[5] J. Heinrich,[31] A. Heiss,[18] M. Herndon,[17] B. Hinrichsen,[23] K. D. Hoffman,[34] C. Holck,[31] R. Hollebeek,[31] L. Holloway,[16] R. Hughes,[27] J. Huston,[25] J. Huth,[14] H. Ikeda,[41] J. Incandela,[10] G. Introzzi,[32] J. Iwai,[43] Y. Iwata,[15] E. James,[24] H. Jensen,[10] M. Jones,[31] U. Joshi,[10] H. Kambara,[13] T. Kamon,[38] T. Kaneko,[41] K. Karr,[42] H. Kasha,[45] Y. Kato,[28] T. A. Keaffaber,[34] K. Kelley,[22] M. Kelly,[24] R. D. Kennedy,[10] R. Kephart,[10] D. Khazins,[9] T. Kikuchi,[41] B. Kilminster,[35] M. Kirby,[9] M. Kirk,[4] B. J. Kim,[19] D. H. Kim,[19] H. S. Kim,[16] M. J. Kim,[19] S. H. Kim,[41] Y. K. Kim,[21] L. Kirsch,[4] S. Klimenko,[11] P. Koehn,[27] A. Köngeter,[18] K. Kondo,[43] J. Konigsberg,[11] K. Kordas,[23] A. Korn,[22] A. Korytov,[11] E. Kovacs,[2] J. Kroll,[31] M. Kruse,[35] S. E. Kuhlmann,[2] K. Kurino,[15] T. Kuwabara,[41] A. T. Laasanen,[34] N. Lai,[7] S. Lami,[36] S. Lammel,[10] J. I. Lamoureux,[4] M. Lancaster,[21] G. Latino,[32] T. LeCompte,[2] A. M. Lee IV,[9] K. Lee,[39] S. Leone,[32] J. D. Lewis,[10] M. Lindgren,[5] T. M. Liss,[16] J. B. Liu,[35] Y. C. Liu,[1] N. Lockyer,[31] J. Loken,[29] M. Loreti,[30] D. Lucchesi,[30] P. Lukens,[10] S. Lusin,[44] L. Lyons,[29] J. Lys,[21] R. Madrak,[14] K. Maeshima,[10] P. Maksimovic,[14] L. Malferrari,[3] M. Mangano,[32] M. Mariotti,[30] G. Martignon,[30] A. Martin,[45] J. A. J. Matthews,[26] J. Mayer,[23] P. Mazzanti,[3] K. S. McFarland,[35] P. McIntyre,[38] E. McKigney,[31] M. Menguzzato,[30] A. Menzione,[32] C. Mesropian,[36] A. Meyer,[7] T. Miao,[10] R. Miller,[25] J. S. Miller,[24] H. Minato,[41] S. Miscetti,[12] M. Mishina,[20] G. Mitselmakher,[11] N. Moggi,[3] E. Moore,[26] R. Moore,[24] Y. Morita,[20] M. Mulhearn,[22] A. Mukherjee,[10] T. Muller,[18] A. Munar,[32] P. Murat,[10] S. Murgia,[25] M. Musy,[40] J. Nachtman,[5] S. Nahn,[45] H. Nakada,[41] T. Nakaya,[7] I. Nakano,[15] C. Nelson,[10] D. Neuberger,[18] C. Newman-Holmes,[10] C.-Y. P. Ngan,[22] P. Nicolaidi,[40] H. Niu,[4] L. Nodulman,[2] A. Nomerotski,[11] S. H. Oh,[9] T. Ohmoto,[15] T. Ohsugi,[15] R. Oishi,[41] T. Okusawa,[28] J. Olsen,[44] W. Orejudos,[21] C. Pagliarone,[32] F. Palmonari,[32] R. Paoletti,[32] V. Papadimitriou,[39] S. P. Pappas,[45] D. Partos,[4] J. Patrick,[10] G. Pauletta,[40]

M. Paulini,[21] C. Paus,[22] L. Pescara,[30] T. J. Phillips,[9] G. Piacentino,[32] K. T. Pitts,[16] R. Plunkett,[10] A. Pompos,[34] L. Pondrom,[44] G. Pope,[33] M. Popovic,[23] F. Prokoshin,[8] J. Proudfoot,[2] F. Ptohos,[12] O. Pukhov,[8] G. Punzi,[32] K. Ragan,[23] A. Rakitine,[22] D. Reher,[21] A. Reichold,[29] W. Riegler,[14] A. Ribon,[30] F. Rimondi,[3] L. Ristori,[32] W. J. Robertson,[9] A. Robinson,[23] T. Rodrigo,[6] S. Rolli,[42] L. Rosenson,[22] R. Roser,[10] R. Rossin,[30] A. Safonov,[36] W. K. Sakumoto,[35] D. Saltzberg,[5] A. Sansoni,[12] L. Santi,[40] H. Sato,[41] P. Savard,[23] P. Schlabach,[10] E. E. Schmidt,[10] M. P. Schmidt,[45] M. Schmitt,[14] L. Scodellaro,[30] A. Scott,[5] A. Scribano,[32] S. Segler,[10] S. Seidel,[26] Y. Seiya,[41] A. Semenov,[8] F. Semeria,[3] T. Shah,[22] M. D. Shapiro,[21] P. F. Shepard,[33] T. Shibayama,[41] M. Shimojima,[41] M. Shochet,[7] J. Siegrist,[21] G. Signorelli,[32] A. Sill,[39] P. Sinervo,[23] P. Singh,[16] A. J. Slaughter,[45] K. Sliwa,[42] C. Smith,[17] F. D. Snider,[10] A. Solodsky,[36] J. Spalding,[10] T. Speer,[13] P. Sphicas,[22] F. Spinella,[32] M. Spiropulu,[14] L. Spiegel,[10] J. Steele,[44] A. Stefanini,[32] J. Strologas,[16] F. Strumia, [13] D. Stuart,[10] K. Sumorok,[22] T. Suzuki,[41] T. Takano,[28] R. Takashima,[15] K. Takikawa,[41] P. Tamburello,[9] M. Tanaka,[41] B. Tannenbaum,[5] W. Taylor,[23] M. Tecchio,[24] P. K. Teng,[1] K. Terashi,[36] S. Tether,[22] D. Theriot,[10] R. Thurman-Keup,[2] P. Tipton,[35] S. Tkaczyk,[10] K. Tollefson,[35] A. Tollestrup,[10] H. Toyoda,[28] W. Trischuk,[23] J. F. de Troconiz,[14] J. Tseng,[22] N. Turini,[32] F. Ukegawa,[41] T. Vaiciulis,[35] J. Valls,[37] S. Vejcik III,[10] G. Velev,[10] R. Vidal,[10] R. Vilar,[6] I. Volobouev,[21] D. Vucinic,[22] R. G. Wagner,[2] R. L. Wagner,[10] J. Wahl,[7] N. B. Wallace,[37] A. M. Walsh,[37] C. Wang,[9] C. H. Wang,[1] M. J. Wang,[1] T. Watanabe,[41] D. Waters,[29] T. Watts,[37] R. Webb,[38] H. Wenzel,[18] W. C. Wester III,[10] A. B. Wicklund,[2] E. Wicklund,[10] H. H. Williams,[31] P. Wilson,[10] B. L. Winer,[27] D. Winn,[24] S. Wolbers,[10] D. Wolinski,[24] J. Wolinski,[25] S. Wolinski,[24] S. Worm,[26] X. Wu,[13] J. Wyss,[32] A. Yagil,[10] W. Yao,[21] G. P. Yeh,[10] P. Yeh,[1] J. Yoh,[10] C. Yosef,[25] T. Yoshida,[28] I. Yu,[19] S. Yu,[31] Z. Yu,[45] A. Zanetti,[40] F. Zetti,[21] and S. Zucchelli[3]

(CDF Collaboration)

[1] *Institute of Physics, Academia Sinica, Taipei, Taiwan 11529, Republic of China*

[2] *Argonne National Laboratory, Argonne, Illinois 60439*

[3] *Istituto Nazionale di Fisica Nucleare, University of Bologna, I-40127 Bologna, Italy*

[4] *Brandeis University, Waltham, Massachusetts 02254*

[5] *University of California at Los Angeles, Los Angeles, California 90024*

[6] *Instituto de Fisica de Cantabria, CSIC-University of Cantabria, 39005 Santander, Spain*

[7] *Enrico Fermi Institute, University of Chicago, Chicago, Illinois 60637*

[8] *Joint Institute for Nuclear Research, RU-141980 Dubna, Russia*

[9] *Duke University, Durham, North Carolina 27708*

[10] *Fermi National Accelerator Laboratory, Batavia, Illinois 60510*

[11] *University of Florida, Gainesville, Florida 32611*

[12] *Laboratori Nazionali di Frascati, Istituto Nazionale di Fisica Nucleare, I-00044 Frascati, Italy*

[13] *University of Geneva, CH-1211 Geneva 4, Switzerland*

[14] *Harvard University, Cambridge, Massachusetts 02138*

[15] *Hiroshima University, Higashi-Hiroshima 724, Japan*

[16] *University of Illinois, Urbana, Illinois 61801*

[17] *The Johns Hopkins University, Baltimore, Maryland 21218*

[18] *Institut für Experimentelle Kernphysik, Universität Karlsruhe, 76128 Karlsruhe, Germany*

[19] *Korean Hadron Collider Laboratory: Kyungpook National University, Taegu 702-701; Seoul National University, Seoul 151-742; and SungKyunKwan University, Suwon 440-746; Korea*

[20] *High Energy Accelerator Research Organization (KEK), Tsukuba, Ibaraki 305, Japan*

[21] *Ernest Orlando Lawrence Berkeley National Laboratory, Berkeley, California 94720*

[22] *Massachusetts Institute of Technology, Cambridge, Massachusetts 02139*

[23] *Institute of Particle Physics: McGill University, Montreal H3A 2T8; and University of Toronto, Toronto M5S 1A7; Canada*

[24] *University of Michigan, Ann Arbor, Michigan 48109*

[25] *Michigan State University, East Lansing, Michigan 48824*

[26] *University of New Mexico, Albuquerque, New Mexico 87131*

[27] *The Ohio State University, Columbus, Ohio 43210*

[28] *Osaka City University, Osaka 588, Japan*

[29] *University of Oxford, Oxford OX1 3RH, United Kingdom*

[30] *Universita di Padova, Istituto Nazionale di Fisica Nucleare, Sezione di Padova, I-35131 Padova, Italy*

[31] *University of Pennsylvania, Philadelphia, Pennsylvania 19104*

[32] *Istituto Nazionale di Fisica Nucleare, University and Scuola Normale Superiore of Pisa, I-56100 Pisa, Italy*

[33] *University of Pittsburgh, Pittsburgh, Pennsylvania 15260*

[34] *Purdue University, West Lafayette, Indiana 47907*

[35] *University of Rochester, Rochester, New York 14627*

[36] *Rockefeller University, New York, New York 10021*

[37] *Rutgers University, Piscataway, New Jersey 08855*

[38] *Texas A&M University, College Station, Texas 77843*

[39] *Texas Tech University, Lubbock, Texas 79409*

[40] *Istituto Nazionale di Fisica Nucleare, University of Trieste/ Udine, Italy*

[41] *University of Tsukuba, Tsukuba, Ibaraki 305, Japan*

[42] *Tufts University, Medford, Massachusetts 02155*

[43] *Waseda University, Tokyo 169, Japan*

[44] *University of Wisconsin, Madison, Wisconsin 53706*

[45] *Yale University, New Haven, Connecticut 06520*

Abstract

We have measured the p_T distribution of top quarks that are pair produced in $p\bar{p}$ collisions at $\sqrt{s} = 1.8$ TeV using a sample of $t\bar{t}$ decays in which we observe a single high-p_T charged lepton, a neutrino and four or more jets. We use a likelihood technique that corrects for the experimental bias introduced due to event reconstruction and detector resolution effects. The observed distribution is in agreement with the Standard Model prediction. We use these data to place limits on the production of high-p_T top quarks suggested in some models of anomalous top quark pair production.

14.65.Ha,13.85.Qk,13.85.Ni

The existence of the top quark has now been established [1–3]. In the standard model, the dominant mechanism for top quark production at the Fermilab Tevatron $p\bar{p}$ Collider is quark-antiquark pair production. However, a number of theoretical investigations [4] have concluded that alternative production mechanisms may play an important role in top production at the Tevatron. In many cases, the kinematic distributions associated with top quark pair production can be significantly modified, so measurement of these distributions can be a sensitive probe of these non-Standard Model phenomena. In particular, many exotic models predict sizeable enhancements in the cross section for the production of top quarks having transverse momentum $p_T > 200$ GeV/c. This letter describes the first measurement of the top quark p_T distribution and provides limits on high-p_T top quark production.

In this analysis, we use a sample of $t\bar{t}$ candidates produced in $p\bar{p}$ collisions at $\sqrt{s} =$ 1.8 TeV and detected with the Collider Detector at Fermilab (CDF). The integrated luminosity of our data sample is 106 pb^{-1}. In the Standard Model, the top quark decays predominantly to a final state consisting of a W boson and a b quark. We consider those $t\bar{t}$ final states where one of the resulting W bosons decays leptonically into either an $e\ \bar{\nu}_e$ or $\mu\ \bar{\nu}_\mu$ pair while the other W boson in the event decays hadronically. This final state and its charge conjugate are known as the "lepton + jets" channel and provide a statistically significant measurement of various $t\bar{t}$ kinematic distributions. We fully reconstruct the lepton + jets events, identify the most likely parton configuration, and use the distribution of reconstructed transverse momenta of the hadronically decaying top candidates as a measure of the top quark p_T distribution.

The Collider Detector at Fermilab is a multipurpose detector, equipped with a charged particle spectrometer incorporating a 1.4 T magnetic field and a finely segmented calorimeter. As particles move outwards from the interaction region, they encounter different detector subsystems that are described in detail elsewhere [5]. Closest to the beam pipe is a silicon vertex detector (SVX). The SVX allows for precise track reconstruction in the transverse plane, and allows for reconstruction of secondary vertices from heavy flavor decays. The momenta of charged particles are measured outside the SVX in an 84-layer drift chamber that extends to a radius of 1.3 m. Outside the tracking system, electromagnetic and hadronic calorimeters in the pseudorapidity [6] region $|\eta| < 4.2$ are used to identify jets and electron candidates. The calorimeters also provide a measurement of the missing transverse energy [7], $\not\!\!E_T$, which can be related to the net transverse energy associated with neutrinos in the final state. In the region $|\eta| < 1.0$ outside the calorimeters, drift chambers provide muon identification. A three-level trigger selects in real time the electron and muon candidates used in this analysis [1]. To improve $t\bar{t}$ detection efficiency, triggers based on $\not\!\!E_T$ are added to the lepton triggers used to collect the first evidence for top quark production.

Two methods are used to identify the bottom hadrons that are produced in top quark decay [2]. The first method, known as SECVTX tagging, relies on identifying secondary vertices arising from the bottom hadron decay by finding two or three tracks that form a vertex displaced from the primary $p\bar{p}$ collision point. The second method, known as soft lepton tagging or SLT, utilizes additional electrons or muons of typically lower p_T than leptons originating from W decay, that result from the semileptonic decay of a heavy quark.

The data samples for this analysis are subsets of inclusive lepton events that contain an isolated electron with $E_T > 20$ GeV or an isolated muon with $p_T > 20$ GeV/c. After the removal of Z boson candidates by rejecting events with two opposite-sign candidate leptons with invariant mass between 75 and 105 GeV/c^2, an inclusive W data sample is made by requiring $\not\!\!E_T > 20$ GeV. We further require that there be at least three jets in the event satisfying the "tight" selection requirements $E_T > 15$ GeV and $|\eta| < 2.0$. This results in a sample of 324 events. In order to ensure that the kinematics of the event are constrained by the measured jet energies, we demand that there be a fourth jet in the event, satisfying the less stringent requirements $E_T > 8$ GeV and $|\eta| < 2.4$. Finally, to increase the signal significance, we demand that either the lowest E_T jet satisfy the tight jet cuts or that at least one jet be tagged by either the SECVTX or SLT algorithm. Eighty-three events pass these selection criteria. Twenty of these events contain jets tagged by the SECVTX algorithm, and fourteen of the remaining sixty-three candidates have an SLT tag.

In order to reconstruct the events, we employ a kinematic fit similar to that used in the measurement of the top quark mass [8]. As opposed to using this fit to measure the top quark mass, we constrain the top quark mass to 175 GeV/c^2, a value close to the world average measurement of this quantity [9]. We assume that the four highest E_T jets correspond to the quarks produced in the decay of the $t\bar{t}$ system. Event reconstruction is complicated by the fact that, in the absence of any b-tagging information, there are 12 different ways to assign these four jets to the four partons of interest. The fit proceeds by varying the input jet energies within their uncertainties. The jet energies used as input to the fit are corrected for calorimeter response, contributions from the underlying events, and particles missed by the jet clustering algorithm. An additional correction is applied to jets assigned to b quarks in the fit to account for differences between the production and decay properties of heavy and light quarks [10].

We reject events having $\chi^2 > 10$ in this three-constraint kinematic fit, leaving 61 events in the data sample. We estimate using a Monte Carlo calculation that after this cut is applied the fraction of $t\bar{t}$ events for which the correct jet-parton assignment is made is approximately 30% for events possessing no b-tags, 40% for events possessing a single b-tagged jet and 60% for events possessing two b-tagged jets. In events for which the incorrect jet-parton assignment is made, there exists only a weak correlation between the measured and true p_T. In Fig. 1 the distribution of measured momenta in HERWIG [11] Monte Carlo samples for top quarks having true p_T's in four different ranges between 0 and 300 GeV/c is depicted. The Monte Carlo calculation that is used to construct these curves, which we shall refer to as our "response functions", includes a simulation of the effects introduced by our reconstruction algorithm and the resolution of the CDF detector. There is a strong correlation between the measured p_T's for the top and anti-top quarks in a given event. Because of this correlation, we perform our measurement of the p_T spectrum using only the fully-reconstructed hadronic top quark decay candidates.

The estimate of the background level in the candidate sample is based on the calculation performed in our measurement of the $t\bar{t}$ production cross section [12]. We correct for differences in the selection criteria between the cross section measurement and the present analysis. The estimated background contribution is 31.9 ± 4.6 events. Events arising from W+jets production are estimated to make up approximately 70% of this background estimate while 20% is expected to originate from QCD multijet production where one jet is misidentified as a lepton [10]. The remaining background comes from a variety of smaller sources such as single top and Z+jets production. We estimate the shape of the background p_T distribution, $V(p_T)$, using a VECBOS Monte Carlo calculation. The VECBOS program [13] is a leading-order matrix element calculation for W+jets production. We show the estimated background distribution in Fig. 2. We have verified, using data samples expected to be enriched in non-W+ jets background, that the VECBOS distribution is an acceptable model for all of the significant backgrounds in our data sample.

The distribution of measured p_T for the 61 events is shown in Fig. 2. To correct for the p_T bias due to the reconstruction and resolution effects illustrated in Fig. 1, we use an unsmearing procedure appropriate for small data samples. This procedure extracts the fraction of top quarks that are produced in each of four p_T bins of width 75 GeV/c, spanning the range between 0 and 300 GeV/c. We perform an unbinned likelihood fit to the measured p_T distribution, using a superposition of our response functions and the background template. The logarithm of the likelihood function that we maximize is

$$\ln[\mathcal{L}] = \sum_{i=1}^{n_{data}} \left\{ \ln \left[\sum_{j=1}^{n_{bin}} ((1-B)R_j T_j(p_T^i)) + BV(p_T^i) \right] \right\} - \frac{(B-\mu_b)^2}{2\sigma^2(\mu_b)} \ . \qquad (1)$$

In this equation, R_j is the fitted fraction of top quarks produced in true bin j, while the $T_j(p_T)$ are the response functions for the $t\bar{t}$ signal and $V(p_T)$ is the background template. The fit parameter B is the fitted background fraction and $\mu_b \pm \sigma(\mu_b)$ is the estimated background fraction. We separate the data into two "tagging subsamples", one of which consists of the subset of events with one or more b tags, the other consisting of those events with no b tags. We fit the subsamples with and without b tags by using forms for the response functions, $T_j(p_T)$, appropriate for the subsample under consideration. This accounts for minor differences in p_T resolution between events possessing one or more b tags and those in the untagged sample. Due to the strong overlap between the signal and background distributions, the effect of incorporating the Gaussian constraint on B is to propagate the background uncertainties into the statistical uncertainty on the R_i.

The response functions $T_j(p_T)$ depend on the form of the true p_T distribution within each p_T bin. Thus, we employ an iterative technique that interpolates the true p_T distribution across a given bin based upon the current R_i parameter values. The fit then uses the results of the previous iteration to construct new response functions. A linear variation within each bin is assumed, and we constrain the true p_T spectrum to go to zero for $p_T = 0$.

We correct the resulting R_i fit values for the fact that the $t\bar{t}$ acceptance is a function of top quark p_T. The relative acceptance in each bin of true p_T is measured using our Monte Carlo calculation and detector simulation. Normalizing the acceptance in the lowest bin of true p_T to 1, the relative acceptance in the subsequent three p_T bins is 1.16 ± 0.01, 1.34 ± 0.02 and 1.24 ± 0.04, where the uncertainties are statistical only.

An important systematic uncertainty in our measurement is associated with the effect of varying the shape of the true p_T distribution within each bin. We estimate the systematic uncertainty arising from this source by measuring the residual bias that remains after the unsmearing is performed. This quantity is estimated by comparing the means of the outcomes of a large number of Monte Carlo "pseudo-experiments" with the expected values for the four R_i's, making various assumptions for the true p_T distribution. We have considered a variety of different true p_T distributions, including distributions whose forms were inspired by Ref. [4]. The largest bias observed for each R_i is taken as a symmetric systematic uncertainty for this parameter. The results of this calculation are shown in Table I.

We estimate the remaining systematic uncertainties, also presented in Table I, using a similar procedure, but where both the response functions and the Monte Carlo pseudo-experiments are generated by assuming the Standard Model p_T distribution. Since we constrain the top quark mass to 175 GeV/c^2, we vary the top quark mass between 170 and 180 GeV [9] and take the largest variation in the means of the R_i for our pseudo-experiments as a systematic uncertainty. Similarly, we estimate the contribution of initial and final state radiation by varying the level of QCD radiation in the PYTHIA Monte Carlo simulation [14] of Standard Model $t\bar{t}$ production. We estimate the systematic uncertainty due to our modeling of the background by varying the Q^2 scale in the VECBOS $W+$ jets Monte Carlo calculation from M_W^2 to $\langle p_T \rangle^2$. Finally, we measure a systematic uncertainty in the acceptance corrections by computing the change in relative acceptance induced by variation of each of the systematic effects detailed above. For each systematic effect, we combine the uncertainties due to changes in the response functions and those due to changes in the relative acceptance corrections by adding the individual uncertainties linearly.

The resulting values for the four R_i are compared to the Standard Model prediction in Table II. We also show the result for $R_1 + R_2$, the fraction of top quarks that are produced with $p_T < 150$ GeV/c (due to a strong negative correlation between the fitted values of R_1 and R_2, the fractional uncertainty in this result is much smaller than it is for the individual estimates for R_1 and R_2). The Standard Model predictions are calculated using the HERWIG Monte Carlo generator and the MRSD0$'$ parton distribution functions [15]. We have also performed a Kolmogorov-Smirnov test for compatibility between the Standard Model prediction and the reconstructed p_T distribution depicted in Fig. 2. Assuming our default Monte Carlo calculation to be correct, the probability to observe a difference between the two distributions as large as the one that is measured is calculated to be 5.0%. This probability varies between 1.0% and 9.4% when the background level and each of the systematic effects are varied by one standard deviation in our model.

We have also calculated a 95% confidence level upper limit on R_4 by combining the statistical and systematic uncertainties using a convolution of the likelihood function for R_4 with a Gaussian distribution, G, that represents the systematic uncertainties. The Gaussian distribution G has a mean value of R_4 and a width equal to the systematic uncertainty in R_4. The result of this calculation is

$$R_4 < 0.16 \text{ at } 95\% \text{ C.L.} \tag{2}$$

This limit has been calculated using the same iterative technique that was used to estimate the four R_i's from the data. This methodology has been shown to produce unbiased results for a wide variety of signal distributions, including those predicted by a number of models [4] of top quark production [16].

We have also searched for top quark production with true $p_T > 300$ GeV/c by modifying our final response function to incorporate a possible high p_T component and subsequently recalculating our upper limit. Since the largest limit is obtained by assuming no high p_T component, we conclude that our upper limit can be extended into a conservative upper limit on the fraction of top quarks produced with p_T in the range 225 to 425 GeV/c. Above this p_T value, we find our relative acceptance for top quarks to begin to fall, reducing to 50% of the acceptance at 225 GeV/c for top quarks produced with $p_T = 500$ GeV/c.

In summary, we have made the first measurement of the top quark p_T distribution. The results are presented in Table II. We have used a likelihood technique to correct for biases introduced due to reconstruction and resolution effects. We have also computed a 95% confidence level upper limit on the fraction of top quarks that are produced with $225 < p_T < 425$ GeV/c, and find that $R_4 < 0.16$ at 95% C.L.

We thank the Fermilab staff and the technical staffs at the participating institutions for their contributions. This work was supported by the U.S. Department of Energy and the National Science Foundation, the Italian Istituto Nazionale di Fisica Nucleare, the Ministry of Science, Culture and Education of Japan, the Natural Sciences and Engineering Research Council of Canada, the National Science Council of the Republic of China, and the A.P. Sloan Foundation.

REFERENCES

[1] F. Abe *et al.*, Phys. Rev. D**50**, 2966 (1994).

[2] F. Abe *et al.*, Phys. Rev. Lett. **74**, 2626 (1995).

[3] S. Abachi *et al.*, Phys. Rev. Lett **74**, 2632 (1995).

[4] C.T. Hill and S.J. Parke, Phys. Rev. D**49**, 4454 (1994); T.G. Rizzo, hep-ph/9902273; E. Simmons hep-ph/hep-ph/9908511; K. Lane, Phys. Rev. **D52**, 1546 (1995).

[5] F. Abe *et al.*, Nucl. Instrum. Methods Phys. Res., Sect. A **271**, 387 (1988); D. Amidei *et al.*, Nucl. Instrum. Methods Phys. Res., Sect A**350**,73 (1994).

[6] We denote by r the radial distance from the beam line and use θ and ϕ to symbolize the polar and azimuthal angles, respectively. The pseudorapidity, η, is defined as $-\ln[\tan(\theta/2)]$. The transverse momentum of a particle with momentum p is $p_T = p\sin\theta$. The transverse energy is $E_T = E\sin\theta$, where E is the particle's energy as measured in the calorimeter.

[7] The missing transverse energy, $\vec{\not\!\!E}_T$ is defined to be $-\sum_i E_T^i\hat{n}_i$, where $\hat{n}_i$ is a unit vector in the azimuthal plane pointing from the beam line to calorimeter tower i.

[8] F. Abe *et al.*, Phys. Rev. Lett. **80**, 2767 (1998).

[9] Particle Data Group, Eur. Phys. J. C **3**, 1 (1998).

[10] F. Abe *et al.*, manuscript in preparation.

[11] G. Marchesini and B.R. Webber, Nucl. Phys. B **310**, 461 (1998); G. Marchesini *et al.*, Comput. Phys. Commun. **67**, 465 (1992). We use HERWIG version 5.6.

[12] F. Abe *et al.*, Phys. Rev. Lett. **80**, 2779 (1998).

[13] F.A. Berends, W.T. Giele, H. Kujif and B. Tausk, Nucl. Phys. B **357**, 32 (1991).

[14] T. Sjöstrand, Comput. Phys. Commun. **82**, 74 (1994).

[15] A.D. Martin, R.G. Roberts, and W.J. Stirling, Phys. Lett. B **308**, 145 (1993).

[16] This methodology does result in a small bias for those signal distributions that concentrate in excess of 80% of the events within the final true p_T bin close to 225 GeV/c. If we allow such unphysical distributions to be candidate theories, the 95% C.L. limit on R_4 rises to 0.19.

TABLES

TABLE I. A summary of the systematic uncertainties. The magnitudes of these uncertainties have been estimated using the means of each measured variable in Monte Carlo pseudo-experiments. These uncertainties have not been scaled by the acceptance correction.

Systematic Effect	δR_1	δR_2	δR_3	δR_4	$\delta(R_1+R_2)$
Top Quark Mass	${}^{+0.026}_{-0.008}$	${}^{+0.000}_{-0.035}$	${}^{+0.039}_{-0.000}$	${}^{+0.000}_{-0.018}$	${}^{+0.010}_{-0.020}$
Initial State Radiation	±0.021	±0.012	±0.011	±0.009	±0.011
Final State Radiation	±0.037	±0.022	±0.009	±0.005	±0.015
Jet Energy Scale	${}^{+0.047}_{-0.020}$	${}^{+0.005}_{-0.043}$	${}^{+0.032}_{-0.000}$	${}^{+0.000}_{-0.016}$	${}^{+0.011}_{-0.023}$
Background Model	±0.025	±0.008	±0.008	±0.010	±0.017
Shape of p_t Spectrum	±0.037	±0.027	±0.051	±0.021	±0.045

TABLE II. The results of our measurement of the top quark p_T distribution. The Standard Model expectation is generated using the HERWIG Monte Carlo program.

p_T Bin	Parameter	Measurement	Standard Model Expectation
$0 \leq p_T < 75$ GeV/c	R_1	$0.21^{+0.22}_{-0.21}(\mathrm{stat})^{+0.10}_{-0.08}(\mathrm{syst})$	0.41
$75 \leq p_T < 150$ GeV/c	R_2	$0.45^{+0.23}_{-0.23}(\mathrm{stat})^{+0.04}_{-0.07}(\mathrm{syst})$	0.43
$150 \leq p_T < 225$ GeV/c	R_3	$0.34^{+0.14}_{-0.12}(\mathrm{stat})^{+0.07}_{-0.05}(\mathrm{syst})$	0.13
$225 \leq p_T < 300$ GeV/c	R_4	$0.000^{+0.031}_{-0.000}(\mathrm{stat})^{+0.024}_{-0.000}(\mathrm{syst})$	0.025
$0 \leq p_T < 150$ GeV/c	R_1+R_2	$0.66^{+0.17}_{-0.17}(\mathrm{stat})^{+0.07}_{-0.07}(\mathrm{syst})$	0.84

FIGURES

FIG. 1. The reconstructed p_T distribution in each of four true p_T bins for Monte Carlo $t\bar{t}$ events. These curves include a simulation of the resolution effects introduced by our reconstruction algorithm and the resolution of the CDF detector. The true p_T distribution within each bin is the HERWIG prediction. This plot includes only the hadronically-decaying top quarks.

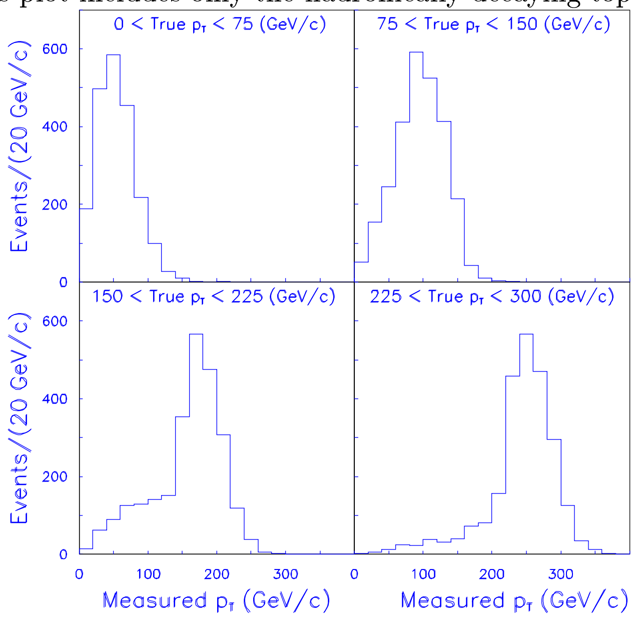

FIG. 2. The measured p_T distribution for the hadronically-decaying top quarks in the 61 event sample. The hatched distribution is the estimated background distribution, normalized to the estimated number of background events. The dashed distribution is the Standard Model prediction, normalized to the observed number of candidate events.